

# SFRC bending behaviour at high temperatures: an experimental investigation

M. Colombo, M. di Prisco & R. Felicetti  
*Politecnico di Milano, Milano, Italy*

**ABSTRACT:** Steel fibre reinforced concrete (SFRC) is increasingly considered as a profitable replacement for diffused reinforcement like welded steel mesh, especially for thin cross sections. In this case fire becomes a very important condition in the design. Previous experimental research showed the benefits in fire resistance of steel fibres when structural elements are bent. A more complete mechanical characterization of the material, when exposed to high temperature, is here presented. The research was instrumental to validate the fire design approach suggested in the recent Italian National Recommendations (CNR-DT 204/06) for design of fibre reinforced concrete structures. Particular attention is given to the reliability of a linear softening constitutive law proposed for uniaxial tension.

## 1 INTRODUCTION

Cementitious composites are typically regarded as brittle materials, with low tensile strength and strain capacity. However with the use of fibre reinforcement, the brittleness shown by plain concrete structures can be overcome producing structures with improved load bearing capacity, ductility and durability. In the last forty years the effect of fibres on toughness, fracture behaviour, impact performance and composite hybridization has been investigated as well as the role of the fibre-matrix interface (di Prisco et al. 2004a).

In the last years new High-Performance cementitious composites have been also developed exhibiting an enhanced elastic limit as well as a strain-hardening response after cracking in bending or even in uniaxial tension (Naaman & Reinhardt 2003).

The material performance improvement and the new applications of these materials ask the researchers to better investigate some new aspects such as fatigue, impact, fire behaviour, durability and shrinkage.

Fire condition is, as a matter of fact, a very important issue in designing precast concrete structures and design in such a condition is now regulated in Europe by European Standard EN 1992-1-2 *Eurocode 2: Design of concrete structure - Part 1.2: General rules - Structural fire design*.

Researchers are very interested in this matter and some open projects are now focused on fire effects on different kind of structures and in particular on

tunnel linings: two large-scale experimental investigations on tunnel lines have been carried out in Austria and in Germany (Dehn & Werther 2006).

The use of steel fibres coupled with polypropylene fibres (Kalifa et al. 2001) can bear some benefits to a structure. The absence of spalling phenomena, first of all, prevents the hot surface to move deeper inside the structure and to reach the inner layers with the consequent mechanical decay of the reinforcement. Steel fibres give to the material a certain residual bending resistance even when exposed to high temperature; this improves the bearing capacity of the structure itself, but it also ensures the conservation of the initial cross section preventing any detachment of external layers.

A recent experimental investigation has shown the benefits given by steel fibre either to mechanical properties of the material at high temperature (di Prisco et al. 2002, di Prisco et al. 2003) and to fire resistance of bent element (di Prisco et al. 2003). In the same research some tests were carried out in order to demonstrate that the mechanical properties of the material does not mainly depend on the temperature at testing, but on the maximum experienced temperature (Colombo et al. 2004). The thermal diffusivity of the material was shown to be scantily affected by steel fibres up to a volume content of 1%.

This research (Colombo 2006) was instrumental to define and validate the fire design approach of the National Recommendation CNR DT204/06 recently issued about the design of fibre reinforced concrete structures in Italy. A proper experimental investiga-

tion is here presented aimed at identifying the material properties after a thermal damage.

## 2 EXPERIMENTAL PROGRAMME

The experimental programme here presented was planned in order to perform a proper identification of the mechanical properties of a steel fibre reinforced concrete (SFRC) and to investigate the stiffness degradation in bending, uniaxial tension and compression when it is exposed to high temperatures. This material is being used for roof elements production in the precast industry.

The material compressive strength is 75 MPa and the fibre content is 50 kg/m<sup>3</sup>; fibres are low-carbon, hooked end, 30 mm long and with an aspect ratio ( $l_f/d_f$ ) equal to 45; all the aggregates are siliceous. The mix design is shown in Table 1.

Table 1. Mix design of steel fibre reinforced concrete.

Constituent	Type	Content	Unit
Cement	I 52.5R	450	kg/m <sup>3</sup>
	0/3	620	kg/m <sup>3</sup>
Aggregates	0/12	440	kg/m <sup>3</sup>
	8/15	710	kg/m <sup>3</sup>
Plasticizer	Acrylic	5.5	kg/m <sup>3</sup>
Total water		195	l/m <sup>3</sup>
Filler		30	kg/m <sup>3</sup>
Fibre		50	kg/m <sup>3</sup>

Twelve prismatic were casted specimens according to National Recommendation UNI 11039.

The thermal treatment of the material was carried out in a oven by performing some thermal cycles up to different maximum temperatures. Three different maximum temperatures (200, 400 and 600°C) were considered. An heating rate equal to 30°C/h was used up to the maximum threshold; after this a 2 hours stabilization phase was imposed in order to guarantee an homogeneous temperature within the specimen. The cooling phase was performed with a rate of 12°C/h down to 200°C, temperature from which the oven was opened in order to faster the natural cooling which tends to slow down approaching the room temperature. In each cycle, three nominally identical specimens were introduced into the oven. In this way all the specimens characterized by the same maximum temperature had the same thermal history. The thermal cycles for the three maximum temperatures considered are summarized in Figure 1.

The experimental programme is organized in three different phases (Fig. 2). The first one refers to the mechanical characterization of the material by means of four point bending tests on notched specimen according to National Recommendation UNI 11039. Once tested, two cylinders 150 mm high with

a 75 mm diameter were cored from each specimen: the first one was tested in uniaxial compression, the second one was notched and tested according to a fixed end uniaxial tension test.

In order to investigate the stiffness degradation of the material, some unloading-reloading cycles were performed in all the tests.

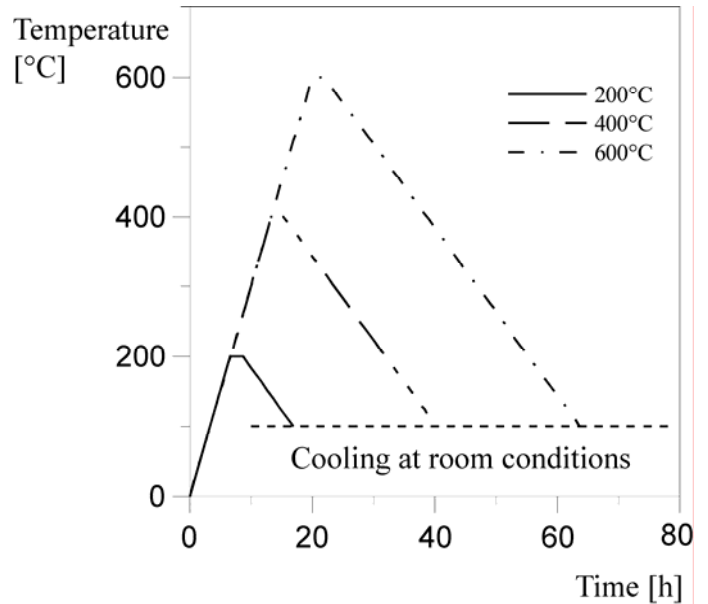


Figure 1: Thermal cycles

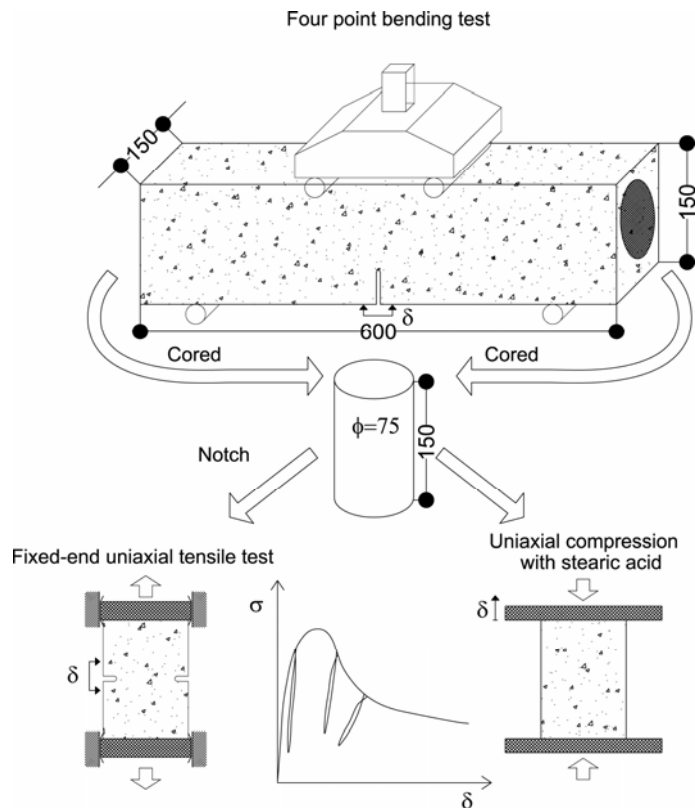


Figure 2 Experimental programme

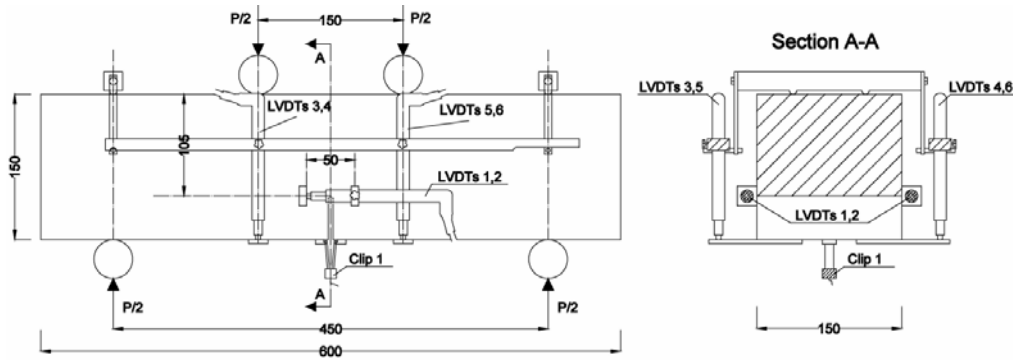


Figure 3: Four point bending test set-up

## 2.1 Four point bending tests

Four point bending tests were performed according to National Recommendation UNI 11039 on 150 x 150 x 600 mm specimens notched with a notch ratio equal to 0.3.

Tests were performed by considering the CMOD measurement (Crack Mouth Opening Displacement, Clip 1) as feedback parameter. In order to measure the crack opening at the notch tip (CTOD) two LVDT transducers were used (LVDTs 1,2). Four different LVDTs were instrumental to measure the deflection under the load application points on both the specimen sides (LVDTs 3-6). In order to prevent that deflection measurements could be affected by crushing of the material at the supports, a proper frame was used (Fig. 3).

The experimental results of four point bending tests are shown in Figure 4 in terms of the nominal stress ( $\sigma_N = 6M / bh^2$ ;  $b$ =width,  $h$ =depth) vs. CTOD curves. The average envelope curves of three nominally identical tests are shown in Figure 5.

Table 2. Four point bending tests nominal stresses: first cracking and average nominal stresses in two different CTOD ranges: 0-0.6 mm and 0.6-3 mm..

Temp.	Test	$f_{If}$ [MPa]	$f_{eq0-0.6}$ [MPa]	$f_{eq0.6-3}$ [MPa]
20°C	1	5.73	5.53	4.18
	2	5.84	4.88	3.29
	<b>Average</b>	<b>5.78</b>	<b>5.21</b>	<b>3.73</b>
	<b>Max x<sub>i</sub> - x̄ </b>	<b>1.04%</b>	<b>6.33%</b>	<b>12.06%</b>
200°C	1	5.79	4.15	3.10
	2	5.57	4.58	3.52
	3	5.47	4.16	3.20
	<b>Average</b>	<b>5.61</b>	<b>4.30</b>	<b>3.27</b>
	<b>Max x<sub>i</sub> - x̄ </b>	<b>3.21%</b>	<b>6.51%</b>	<b>7.65%</b>
400°C	1	2.91	2.98	1.50
	2	2.31	2.66	1.44
	3	2.78	3.07	2.27
	<b>Average</b>	<b>2.67</b>	<b>2.90</b>	<b>1.74</b>
	<b>Max x<sub>i</sub> - x̄ </b>	<b>13.48%</b>	<b>8.28%</b>	<b>30.46%</b>
600°C	1	3.01	2.69	1.52
	2	2.80	2.67	2.04
	3	2.63	2.60	1.00
	<b>Average</b>	<b>2.81</b>	<b>2.65</b>	<b>1.52</b>
	<b>Max x<sub>i</sub> - x̄ </b>	<b>7.12%</b>	<b>1.89%</b>	<b>34.21%</b>

The mechanical strengths at increasing temperature are listed in Table 2 and plotted in Figure 6. The meaning of each parameter can be explained as follows:

$f_{If}$ : first cracking strength representing the matrix tensile strength; it's the nominal stress corresponding to a CTOD equal to 25  $\mu$ m;

$f_{eq0-0.6}$ : average nominal strength in the CTOD range between 0.025 mm and 0.625 mm representing the Serviceability Limit State (SLS) residual strength;

$f_{eq0.6-3}$ : average nominal strength in the CTOD range between 0.625 mm and 3.025 mm representing the Ultimate Limit State (ULS) residual strength, when material behaviour is governed only by pull-out mechanism.

Looking at the experimental results, a remarkable decay of material properties between 200°C and 400°C is observed; for higher temperatures the material properties seem to remain quite constant; for temperatures lower than 200°C the first cracking nominal strengths do not seem to be affected by thermal treatment.

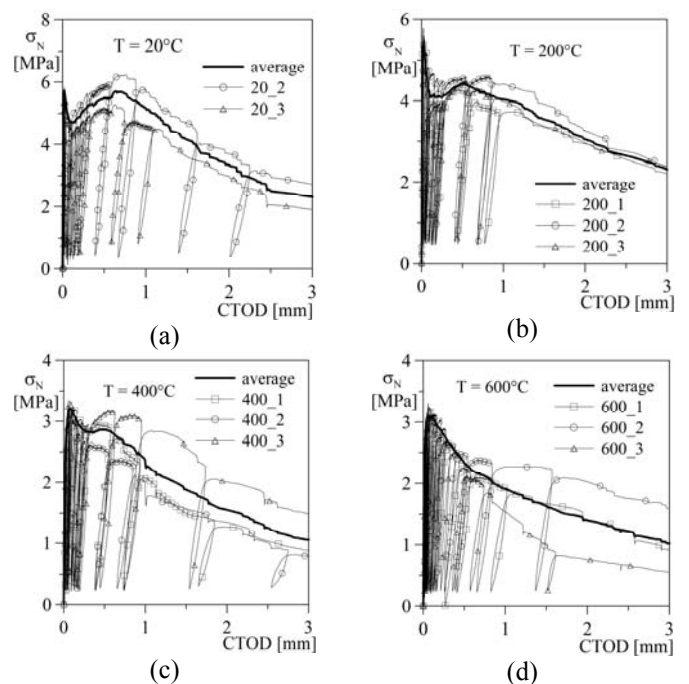


Figure 4: Four point bending tests results: nominal stress vs. CTOD curves for different temperatures (a) T=20°C, (b) T=200°C, (c) T=400°C, (d) T=600°C.

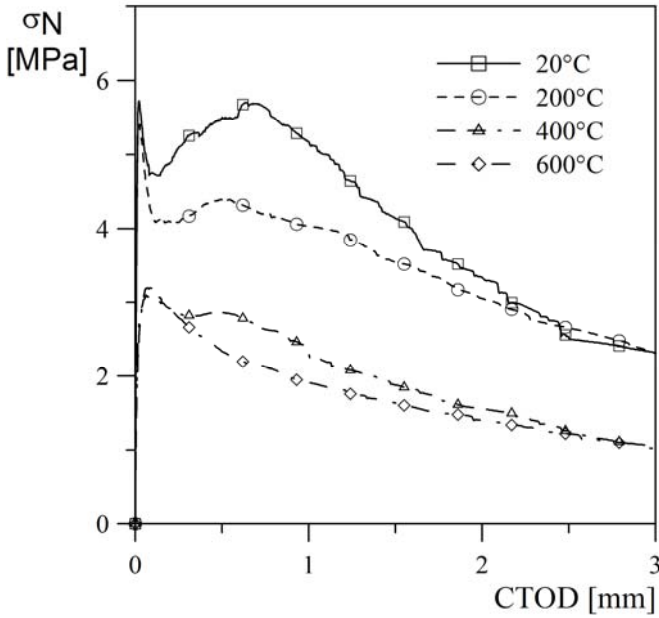


Figure 5: Four point bending tests: envelope average nominal stress vs. CTOD curves

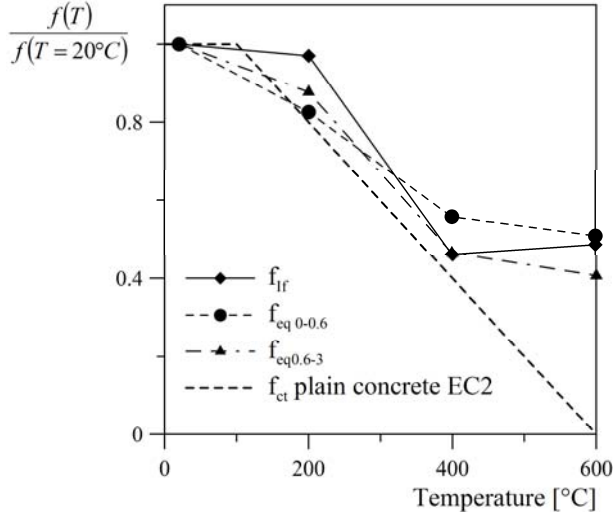


Figure 6: Four point bending tests: nominal stress behaviour with temperature.

## 2.2 Uniaxial compression tests

Uniaxial compression tests were performed on cylinders cored from the beam after bending test. Specimens were instrumented by means of seven LVDT transducers: three disposed at  $120^\circ$  around the specimen in order to measure the displacement between the loading platens of the press, other three LVDTs, disposed at  $120^\circ$  as well, were applied to the central zone of the specimen with a gauge equal to 50 mm; finally one LVDT connected to a chain surrounding the specimen was used to measure the average circumferential relative displacement in the central region. The geometry and the specimen set-up in uniaxial compression are shown in Figure 7.

In order to reduce friction with the press platens some stearic acid was smeared on the specimen ends.

All the tests were displacement controlled by using as feedback parameter the total vertical displacement of the specimen measured by one of the full bridge LVDT.

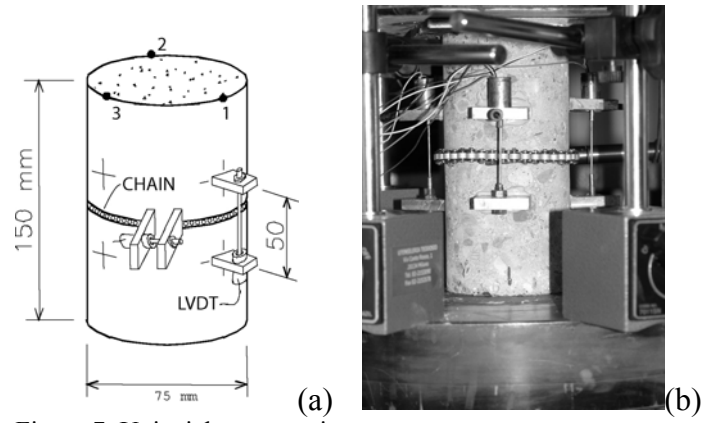


Figure 7: Uniaxial compression test set-up

Table 3. Uniaxial compression tests: peak nominal strengths.

Temperature	Test	Peak nominal strength [MPa]
20°C	2	79.25
	3	70.70
	<b>Average</b>	<b>74.98</b>
	<b>Max x<sub>i</sub> - x̄ </b>	<b>5.71%</b>
200°C	1	60.26
	2	64.81
	3	60.89
	<b>Average</b>	<b>61.99</b>
	<b>Max x<sub>i</sub> - x̄ </b>	<b>4.55%</b>
400°C	1	59.52
	2	56.46
	3	60.02
	<b>Average</b>	<b>58.67</b>
	<b>Max x<sub>i</sub> - x̄ </b>	<b>3.77%</b>
600°C	1	44.98
	2	57.57
	3	38.20
	<b>Average</b>	<b>46.92</b>
	<b>Max x<sub>i</sub> - x̄ </b>	<b>22.70%</b>

The displacement rate imposed was equal to 0.1 mm/min either in loading and unloading phases.

The experimental results are shown in Figure 8 by means of the nominal stress ( $\sigma_N = P/A$ ) vs. normalized total vertical displacement ( $\delta/l$ ) curves.

In testing specimens at room condition some instabilities in controlling the test caused in two cases a sudden failure before reaching the peak load. The variation of peak nominal strength is summarized in Table 3 and Figure 9; in compression tests, differently from what happened in bending, the degradation of the material is quite linear in all the temperature range investigated, even if in the range between 200°C and 400°C the peak nominal strength seems to be less influenced by temperature increasing.

The behaviour experimentally detected is similar to the one proposed by Eurocode 2 for plain concrete (Fig. 9).

The average envelope behaviour of the material, for different maximum temperatures, is shown in Figure 10.

In this figure the nominal stress is respectively plotted with respect on the left side, to the normalized total vertical

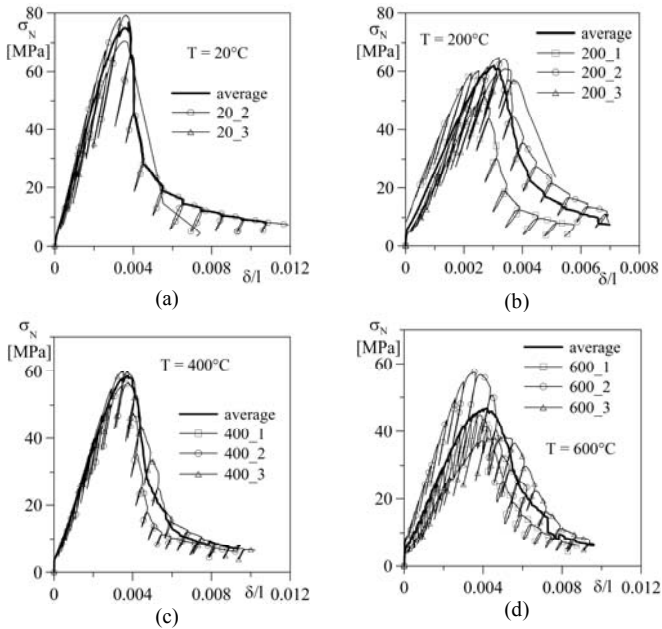


Figure 8: Uniaxial compression tests: nominal stress vs. normalized vertical displacement curves for different temperatures (a)  $T=20^{\circ}\text{C}$ , (b)  $T=200^{\circ}\text{C}$ , (c)  $T=400^{\circ}\text{C}$ , (d)  $T=600^{\circ}\text{C}$ .

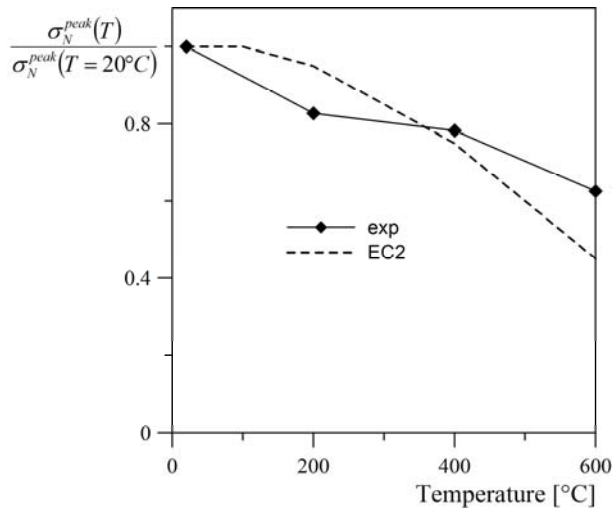


Figure 9: Uniaxial compressive tests: peak nominal strength at different temperatures.

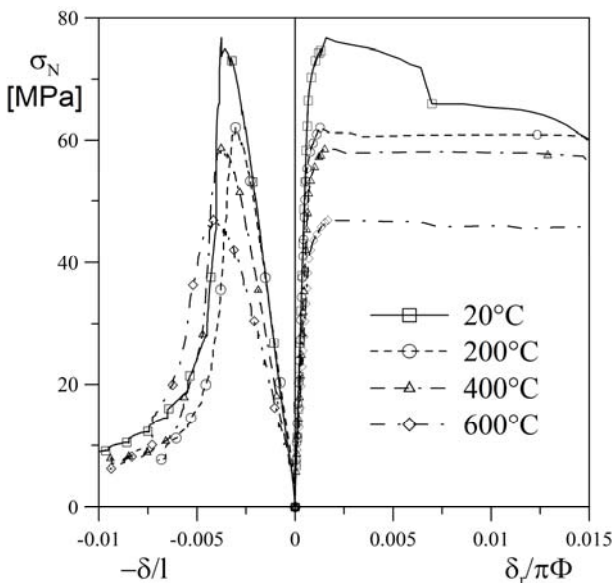


Figure 10: Uniaxial compression tests: envelope average curves.

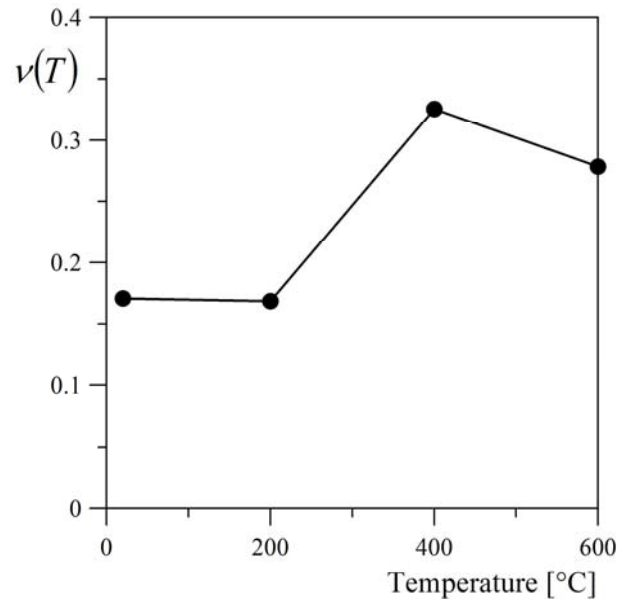


Figure 11: Poisson ratio evolution

displacement ( $\delta/l$ ) and on the right side to the normalized circumferential displacement. In the latter case the circumferential displacement ( $\delta_r$ ), read from the transducer placed on the chain clamped on the specimen, is divided by the perimeter of the cylinder cross section ( $\pi\phi$ ).

Comparing the normalized circumferential displacement with the total vertical one the evolution of Poisson's ratio at increasing temperature can be detected by taking into account the ratio between these two quantities in the initial elastic branch of each curve in the range between 5% and 30% of the peak load. The evolution of the Poisson ratio is represented in Figure 11; the main contribution of temperature occurs in the range between  $200^{\circ}\text{C}$  and  $400^{\circ}\text{C}$ .

### 2.3 Fixed end uniaxial tension tests

Uniaxial tension tests were performed on notched cylinders (Fig. 12) glued to the press platens by means of an epoxy glue made of two components: binder and hardener. The specimen was instrumented by six displacement transducers LVDTs: three were placed astride the notch (gauge length = 50 mm) to measure crack opening displacement (COD) and three were used to measure the displacement between the two end platens of the press. One of the latter was used as the feedback parameter in performing tests. The displacement rate imposed during the tests was equal to  $0.04 \mu\text{m/s}$  either in loading and unloading branch up to crack opening displacement equal to 0.6 mm and was then increased to  $0.4 \mu\text{m/s}$  for higher COD.

In order to keep the platens parallel during the test an active control was performed (Fig.12). Four steel 14 mm diameter bars were used to connect the fixed base of the press with the upper plate

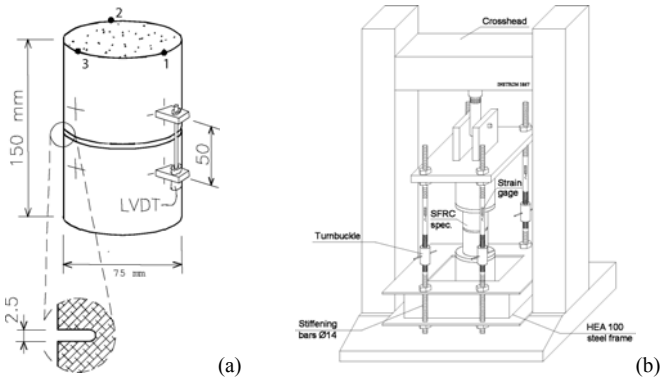


Figure 12: Uniaxial tensile test set-up

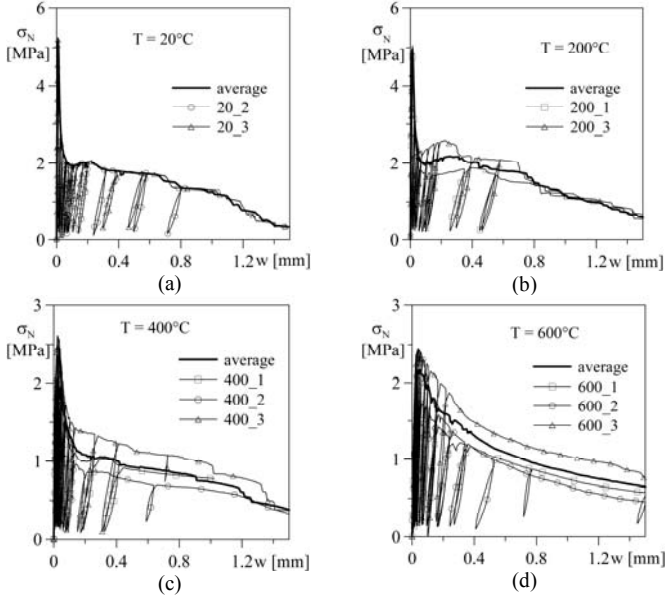


Figure 13: Uniaxial tensile tests: nominal stress vs. crack opening displacement ( $w$ ) curves for different temperatures (a)  $T=20^\circ\text{C}$ , (b)  $T=200^\circ\text{C}$ , (c)  $T=400^\circ\text{C}$ , (d)  $T=600^\circ\text{C}$ .

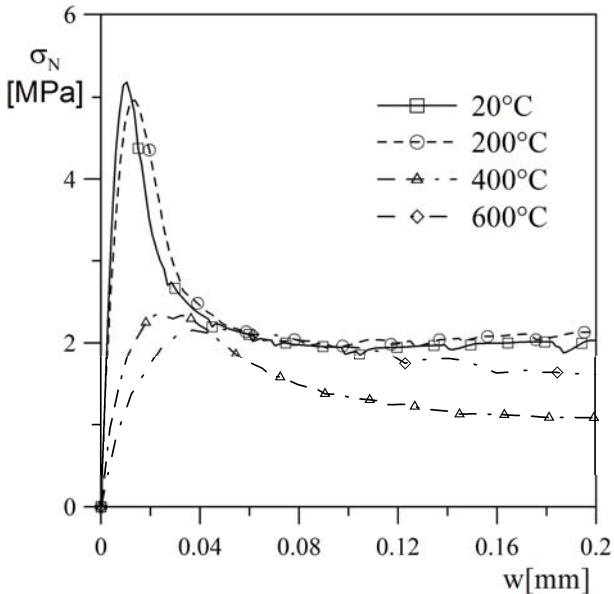


Figure 14: Uniaxial tensile tests: envelope average curves.

connected to the specimen and to an articulated joint. The bars were fixed to a steel frame made of HEA100 beams connected to the basement of the press. These bars have an adjustable length by means of a turnbuckle and each bar is instrumented with two strain-gages to measure its elongation. Acting on the turnbuckles during the tests it was ensured that all the crack opening measurements were very close in order to consider the plates as fixed.

This test set-up induces in the specimen also a bending moment: the maximum value reached in both direction ( $x$  and  $y$ ) was equal to  $0.15 \text{ kNm}$  to which correspond the maximum rotation  $\vartheta_x^{\max} = 1.31 \cdot 10^{-5}$  and  $\vartheta_y^{\max} = 7.40 \cdot 10^{-6}$ .

The experimental results are shown in Figure 13 by means of nominal stress ( $\sigma_N = P/A$ ) vs. crack opening displacement ( $w$ ) curves.

In performing two tests (one at room condition and one at  $200^\circ\text{C}$ ) some problems occurred in controlling the press: this caused these two tests to be lost. The envelope average curves  $\sigma_N$  vs.  $w$  are shown in Figure 14. In order to better investigate the uniaxial tensile behaviour of SFRC when exposed to high temperatures the evolution of two different nominal strength is considered:

$\sigma_N^{\text{peak}}$ : nominal stress at peak that represents the matrix behaviour;

Table 4. Uniaxial tensile tests: nominal stress at peak and average nominal stresses in COD range:  $0.9 \text{ mm} \pm 20\%$ .

Temperature	Test	$\sigma_N^{\text{p}}$ [MPa]	$\sigma_N^{0.9}$ [MPa]
20°C	1	5.21	1.32
	2	5.27	1.32
	<b>Average</b>	<b>5.24</b>	<b>1.32</b>
	<b>Max x<sub>i</sub> - x̄ </b>	<b>0.57%</b>	<b>0.16%</b>
200°C	1	5.06	1.30
	2	4.92	1.30
	<b>Average</b>	<b>4.99</b>	<b>1.30</b>
	<b>Max x<sub>i</sub> - x̄ </b>	<b>1.4%</b>	<b>0.11%</b>
400°C	1	2.61	-
	2	2.06	0.65
	3	2.47	0.99
	<b>Average</b>	<b>2.38</b>	<b>0.82</b>
<b>Max x<sub>i</sub> - x̄ </b>	<b>13.45%</b>	<b>20.73%</b>	
600°C	1	1.73	0.80
	2	2.46	0.71
	3	2.37	1.09
	<b>Average</b>	<b>2.19</b>	<b>0.87</b>
<b>Max x<sub>i</sub> - x̄ </b>	<b>21.00%</b>	<b>25.29%</b>	

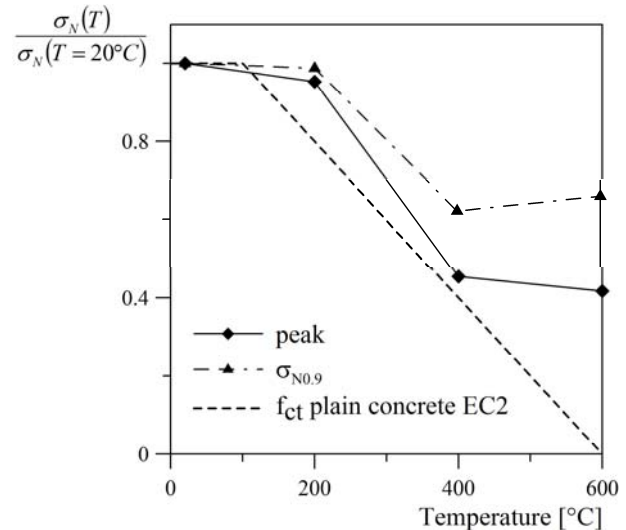


Figure 15: Uniaxial tensile tests: nominal stress at peak and average nominal stresses in COD range:  $0.9 \text{ mm} \pm 20\%$ .

$\sigma_N^{0.9}$ : average nominal stress in the crack opening displacement ( $w$ ) range  $0.9 \pm 20\%$  related to pull-out mechanism.

The evolution of these two parameters is summarized in Table 4 and shown in Figure 15. As already seen in the bending behaviour the highest material degradation occurs in the temperature range between  $200^\circ\text{C}$  and  $400^\circ\text{C}$ ; out of this range the nominal stresses considered are quite constant. The pull-out mechanism seems to increase the strengths between  $400^\circ\text{C}$  and  $600^\circ\text{C}$ ; this behaviour is similar to the one observed in a previous experimental investigation (di Prisco et al. 2003b) on a nominally identical material.

### 3 UNIAXIAL TENSILE CONSTITUTIVE LAW

The knowledge of the uniaxial constitutive law is a very important issue in the design of steel fibre reinforced concrete structures. The new National recommendation CNR DT 204/06 propose for fibre reinforced concrete the linear softening stress ( $\sigma$ ) – crack opening relationship shown in Figure 16.

The linear softening law recommends the identification of two stress parameter ( $\sigma_a$  and  $\sigma_b$ ) by means of four point bending tests according to UNI 11039. These stress parameters are defined according to the following formulation:

$$\sigma_a = 0.45 \cdot f_{eq0-0.6}$$

$$\sigma_b = 0.5 \cdot f_{eq0.6-3} - 0.2 \cdot f_{eq0-0.6}$$

The constitutive law proposed is aimed to describe the behaviour of the material governed by fibre pull-out mechanism, neglecting in the design procedure the matrix strength and the unstable crack propagation in the concrete matrix.

The National Recommendation proposes the same uniaxial tension constitutive law also in fire condition, providing a proper identification procedure to be performed by means of four point bending tests on specimens damaged by a thermal cycle. This procedure uses tests at room condition, computes the residual equivalent strengths  $f_{eq0-0.6}$  and  $f_{eq0.6-3}$  in specimen previously subjected at different maximum temperature reached during a thermal cycle.

The reliability of the constitutive law, also at high temperatures, is shown in Figure 17 where the constitutive law identified from bending tests performed at different maximum temperatures ( $T_{max} = 20, 200, 400$  and  $600^\circ\text{C}$ ) are compared with the experimental results of the uniaxial tensile tests performed on cylindrical specimens cored from the same beam on which the bending tests was carried out.

Looking at the tensile behaviour governed by fibre pull-out mechanism, all the cases investigated show a good reliability of the uniaxial constitutive law proposed; the only exception is observed for

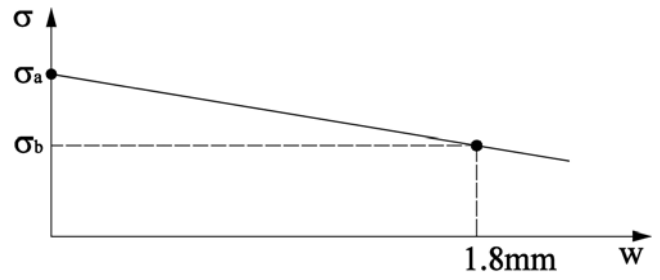


Figure 16: Uniaxial tension linear constitutive law.

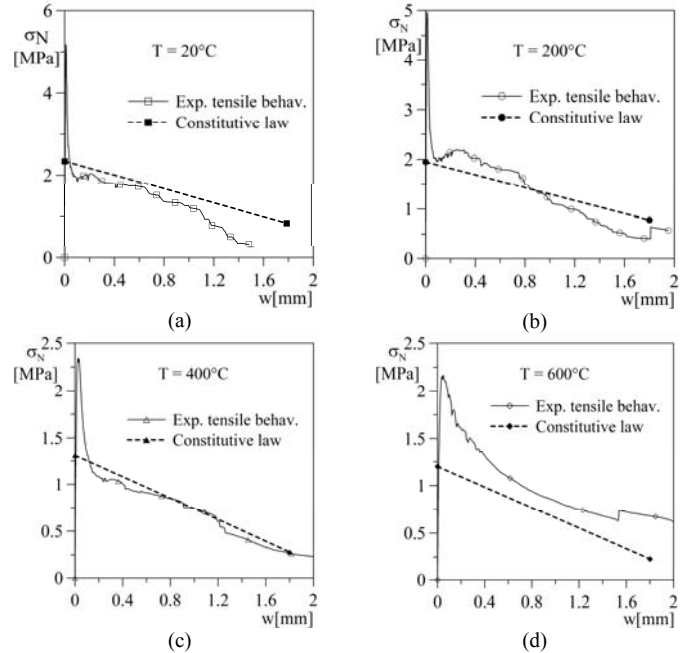


Figure 17: Uniaxial tensile behaviour: constitutive law validation (a)  $T=20^\circ\text{C}$ , (b)  $T=200^\circ\text{C}$ , (c)  $T=400^\circ\text{C}$ , (d)  $T=600^\circ\text{C}$  in term of average curves.

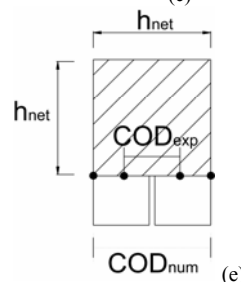
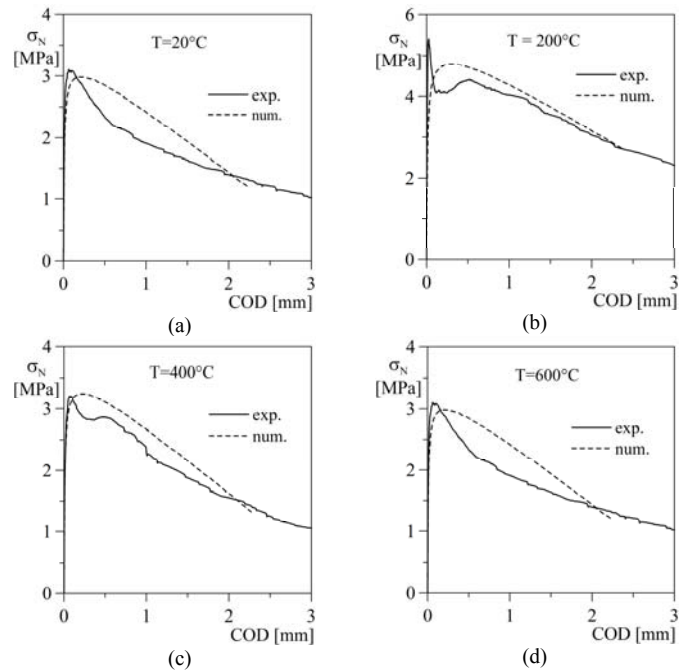


Figure 18: Bending behaviour: numerical prediction (a)  $T=20^\circ\text{C}$ , (b)  $T=200^\circ\text{C}$ , (c)  $T=400^\circ\text{C}$ , (d)  $T=600^\circ\text{C}$ . (e) Notation in COD definition

$T_{\max}=600^{\circ}\text{C}$  where the scatter is equal to 20%. It's worth noting that, in this last case, the constitutive law is in favour of safety.

#### 4 DESIGN PREDICTIONS

In this section the bending behaviour of the material previously investigated is taken into account (di Prisco et al. 2003a,b). The case of bent elements in which the element cross section is characterized by a uniform thermal damage (Colombo & di Prisco 2006) is taken into account by considering the design approach suggested by National Recommendation and just explained.

Considering the situation of uniformly distributed thermal damage, the comparison between the experimental tests previously described and the numerical predictions is shown in Figure 18 for the different temperatures considered. The numerical simulations were performed by considering the plane section assumption (di Prisco et al. 2004b) according to the multi-layer procedure proposed by Hordijk (1991). In this way, the notch effect was neglected and the net section of the specimen was assumed as critical section.

Good results are achieved also taking into account the simplicity of the constitutive law and of the approach considered. In all the cases investigated the local scatter in terms of nominal stress is lower than 20%.

#### 5 CONCLUDING REMARKS

The research here presented is the final step of a long research programme of about three years aimed to evaluate fire resistance of fibre reinforced concrete structure with a fibre content lower than 1%. This research allowed us to conclude that is possible to perform a mechanical identification at room condition after thermal cycles characterized by a maximum temperature that causes an irreversible thermal damage of the material. The thermal diffusivity is not significantly affected by the fibres content considered. In order to design steel fibre reinforced concrete structures in fire conditions is possible to adopt a linear constitutive softening law to describe the post-peak uniaxial tensile behaviour and to use a simply plane section model. This conclusion moved the fire design approach suggested by the recent National Recommendation CNR DT 204/06.

#### 6 ACKNOWLEDGMENTS

The authors thank Magnetti Larco-Building for the technical support in the cast of the specimens. The

research was financially supported by the Italian Ministry for the Education, University and Research (PRIN 2004).

#### REFERENCES

- CNR DT204. 2006. Instruction for Design Execution and Control of Fibre Reinforced Concrete Structures (in Italian).
- Colombo, M, Felicetti, R., Manzoni, M. & Bergamini, E. 2004. On the bending behaviour of SFRC exposed to high temperature. In di Prisco, Felicetti & Plizzari (eds.), *Proc. Of 6th Symposium on Fibre Reinforced Concrete BEFIB 2004 – PRO39*: 647-658. Bagnaux, France: RILEM Publications S.A.R.L.
- Colombo, M. 2006. FRC bending behaviour: a damage model for high temperatures. *Ph.D. Thesis, Department of Structural Engineering, Politecnico di Milano, Italy*.
- Colombo, M & di Prisco, M. 2006. SFRC: a damage model to investigate the high temperature mechanical behaviour. In Meschke, de Borst, Mang & Bicanic (eds.), *Computational Modelling of Concrete Structures EURO-C*: 309-318. Rotterdam: Balkema.
- Dehn, F. & Werther, N. 2006. Brandversuche an Tunnel-schalenbetonen für den M30-Nordtunnel in Madrid (Fire tests on tunnel concretes for the M30-Northtunnel in Madrid). *Beton- und Stahlbetonbau* 9: 729-731 (in German).
- di Prisco, M., Felicetti, R. & Gambarova, P. 2003a. On the fire behavior of SFRC and SFRC structures in tension and bending. In A.E. Naaman & H.W. Reinhardt (eds.), *High Performance Fiber Reinforced Cement Composite*: 205-220. Bagnaux, France: RILEM Publications S.A.R.L.
- di Prisco, M., Felicetti, R. & Colombo, M. 2003b. Fire resistance of SFRC thin plates. In Bicanic, de Borst, Mang & Meschke (eds.), *Computational Modelling of Concrete Structures EURO-C*: 783-792. Rotterdam: Balkema.
- di Prisco, M., Felicetti, R. & Plizzari, G. (eds.) 2004a. *Proc. Of 6th Symposium on Fibre Reinforced Concrete BEFIB 2004 – PRO39*. Bagnaux, France: RILEM Publications S.A.R.L.
- di Prisco, M., Ferrara, L., Colombo, M. & Mauri, M. 2004b. On the identification of SFRC constitutive law in uniaxial tension. In di Prisco, Felicetti & Plizzari (eds.), *Proc. Of 6th Symposium on Fibre Reinforced Concrete BEFIB 2004 – PRO39*: 827-836. Bagnaux, France: RILEM Publications S.A.R.L.
- EN 1992-1-2. 2002. Eurocode 2: Design of concrete structure – Part 1.2: General rules – Structural fire design.
- Hordijk, D. 1991. Local approach to fatigue of concrete. *Ph.D. Thesis, Department of Concrete Structures, Faculty of Civil Engineering, Delft University of Technology, The Netherlands*:131-134.
- Kalifa, P., Chene, G. & Galle, C. 2001. High temperature behaviour of HPC with polypropylene fibres. From spalling to microstructure. *Cement and concrete research* 31: 1487-1499.
- Naaman, A.E. & Reinhardt, H.W. (Eds.) 2003 *High Performance Fiber Reinforced Cement Composites (HPFRCC4)* - RILEM PRO 30. Bagnaux, France: RILEM Publications S.A.R.L.
- UNI 11039. 2003. Concrete reinforced with steel fibres. Part II Test method for the determination of first cracking strength and ductility indexes (in Italian).